Comparison of analytical and numerical solution of bearing contact analysis

Peter Šulka[1,*], *Alžbeta Sapietová*[1], *Vladimír Dekýš*[1], and *Milan Sapieta*[1]

[1]Department of Applied Mechanics, Faculty of mechanical engineering, University of Žilina, Univerzitná 8215/1, 010 26 Žilina, Slovak Republic

Abstract. In this paper, an effort has been put to analyze the rolling ball bearing using finite element analysis the contact pressure level, stress or displacement behavior of rolling ball bearing. The obtained results were then compared with the analytical results obtained through the methodology of Hertz theory, which means composition and solution of analytical formulas and equations based on specific ball bearing parameters in order achieve optimal results to demonstrate an almost identical similarity of results of numerical and analytical solution and correct setting up of the given simulation in computational software ANSYS Workbench.

Keywords: static structural analysis, contact, Hertz theory, ANSYS Workbench

1 Introduction

Rolling bearings are among the most important components of conveyor belts, working machines or various rotary mechanical applications and, therefore, the trend of increasing demands in terms of their production, accuracy, load-bearing capacity and reliability is increasing.

Their application lies in all branches of industry, from the production of heavy duty machinery in mining and stamping, in all modes of transport or in automotive or aviation, to the application of miniature bearings to high speed dental drills.

First of all, who drew and invented the ball-bearings was Leonardo da Vinci around the year 1500. He designed the ball bearings to be incorporated into his design for the helicopter – it would make rotating the large screw on top much easier by reducing the friction by several orders of magnitude. Philip Vaughan invented the ball bearing in the year 1794, it was 294 years after Leonardo´s design. Vaughan´s patent described how iron balls could be placed between the wheel and the axle and carriage. The balls let the carriage wheels rotate freely by reducing friction. Later, in August 1869, Parisian bicycle mechanic Jules Suriray received the first French patent for ball bearings. The bearings were then fitted to the winning

* Corresponding author: peter.sulka@fstroj.uniza.sk

Reviewers: *Zbigniew* Kłos, *Milan* Žmindák

bicycle ridden by James Moore in the world´s first bicycle road race. The modern, self-aligning design of the ball bearing is attributed to Sven Wingquist of the SKF ball-bearing manufacturer in 1907. In the year 2002 INA/FAG established by Dr. Georg Schaeffler and Dr. Wilhelm Schaeffler E1 spherical ball and roller bearing, which is base of current, modern rolling bearings [1-3].

Rolling bearings allow for the transfer of forces between the moving and fixed parts of the mechanical system and are designed to minimize friction arising from power and energy transfer.

Due to their multiple use, increasing emphasis is placed on their development and improvement, because in many cases the bearings do not provide the required durability according to the calculation values. There may be many reasons, for example, overload, load lower than required, inadequate lubrication, ineffective sealing, inadequate over fitting, or impact load on the bearing that leads to permanent deformation in the form of imprints in the bearing ring path paths. This very latest case of damage is becoming more and more frequent, for example automobile chassis bearings and it is necessary to examine the problem in order to examine the given load condition using the FEM method and to obtain optimal results for further research and modification of bearings with the intention of eliminating impact damage. Researchers still continue with the intensive development and research in field of rolling bearings with purpose to investigate new theory of bearing aspects, solving significant parameters and values of rolling bearings in order to ensure maximum quality and accurate prediction [4-5].

2 The contact state analysis and theoretical computation for rolling ball bearing

When the rolling ball bearing works, it is usually that more than one rolling ball bears the load. The condition is complex between rollers and rings. When the load is 0, contact area is a point, i.e., point-contact. When the load increases in running, the bearing inner ring, outer ring and rolling elements bring forth plastic deformation in the contact area, so the point-contact becomes face-contact. Furthermore, contact area gradually becomes ellipse, and generates residual stress. The contact parameters, such as the place, size, shape of contact area, as well as the contact pressure and friction force distribution, will be variable with the loads changing. These facts are typical boundary conditions for nonlinear problems.

When any two curved bodies of different radii of curvature are brought into contact they will initially touch at either a point or along a line. With the application of the smallest load, elastic deformation enlarges these into contact areas across which the loads are distributed as pressures. The first analysis of the situation was presented by Heinrich Hertz in 1881 and is based on the following assumptions [6].

1. The surfaces are continuous, smooth, nonconforming and frictionless,
2. The size of the contact are is small compared to the size of the bodies, i.e., the strains associated with the deformations are small.
3. Each solid can be considered to behave as an elastic half-space in the vicinity of the contact zone.

Although strictly, previous idealizations require parabolic surface profiles, by implication Hertzian analysis is relevant to the contact of spheres, cylinders, and ellipsoids. Progress over the last century in contact mechanics can be seen as the gradual relaxation of the restrictions imposed by the original Hertzian treatment, for an exhaustive review, see Johnson (1985) [7].

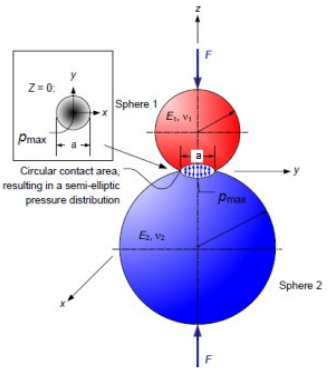

Fig. 1. Hertzian theory illustrated contact between two spheres [2]

From the Fig. 1 is possible to detect significant parameter a, which is defined as wide of contact area. In case of point contact, the maximum contact pressure (see Fig. 2) is situated in the middle of contact area with appropriate value defined by equation (Eq. 1 or Eq. 11) [8, 9].

$$p_{max} = \frac{3W}{2\pi ab} \tag{1}$$

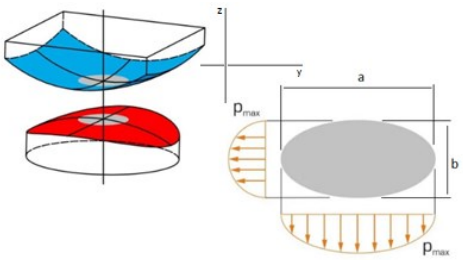

Fig. 2. The elliptical contact pressure

3 Contact pressure in the rolling ball bearing by using the Hertzian theory/analytical solution

The maximum pressure computation was performed by using the following relationships dependent on bearing parameters, external load and mathematical coefficients. External load was defined for value IF= 10,000 N according to the empirical formula (Eq. 2), which depends on constructional and physical properties of specific vehicle, wheel drive and rolling ball bearing (see Fig. 3).
The formula (Eq. 2) is based on generally known and experimentally found parameters:

$$IF = \left((-55.2 + 0.0081 * GAW + 7.81 * 5 + 0.012 * COG + 0.118 * SLR) * EF\right) \tag{2}$$

where:
IF – is the value of external load,
GAW – is the axle load [kg],
COG – is the height of center of vehicle gravity [mm],
SLR – is the dynamical radius [mm],
EF – is the empirical factor found through the experiments.

Analytical solution of ball bearing contact pressure depends on parameters shown in Tab. 1:

Table 1. Proposed parameters of ball bearing for analytical calculation

Parameter	Symbol	Value	Unit
Poisson´s ratio of ball	V_1	*0.29*	---
Poisson´s ratio of race	V_2	*0.29*	---
Elastic modulus of ball	E_1	*210*	*GPa*
Elastic modulus of race	E_2	*210*	*GPa*
Radius of ball	R_1	*10*	*mm*
Inner race radius	R_2	*10.2*	*mm*
Inner race radius	R_3	*35*	*mm*
Maximum load on bearing ball	*IF*	*10000*	*N*

The solution is intended by the section of following formulas and equations [10].

$$a = 1.145 \cdot n_a \cdot (IF \cdot K \cdot \gamma)^{1/3} \tag{3}$$

$$b = 1.145 \cdot n_b \cdot (IF \cdot K \cdot \gamma)^{1/3} \tag{4}$$

a is the semimajor axis of contact ellipse,
b is the semiminor axis of contact ellipse.

$$n_c = \frac{1}{E(e)} \cdot \left(\frac{\pi^2 \cdot k \cdot E(e)}{4}\right)^{1/3} \tag{5}$$

$$E(e) = \int_0^{\pi/2} \sqrt{1 - e^2 \cdot sin^2(\varphi) d\varphi} \tag{6}$$

$$k = \frac{a}{b} \tag{7}$$

$$e = \sqrt{1 - \left(\frac{b}{a}\right)^2} \tag{8}$$

E(e) is the elliptical intergral.

$$K = \frac{1}{\frac{2}{R_1} - \frac{1}{R_2} + \frac{1}{R_3}} \tag{9}$$

$$\gamma = \frac{(1 - {v_1}^2)}{E_1} + \frac{(1 - {v_2}^2)}{E_2} \tag{10}$$

$$P_{Hertz} = 0.365 \cdot n_c \cdot \left[\frac{IF}{K^2 * \gamma^2}\right]^{\frac{1}{3}} = 2569\ MPa \tag{11}$$

P_{Hertz} is the maximum contact pressure according to the Hertz theory.

From these empirical relations, the maximum contact pressure was determined to the value P_{Hertz} = 2569 MPa, a = 5.155 mm and b = 0.361 mm.

4 Numerical solution of maximum contact pressure by using Finite element method/numerical solution

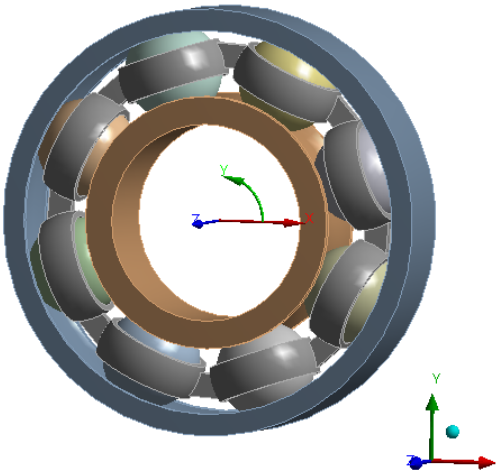

Fig. 3. 3D model of investigated rolling ball bearing

The FEM analysis was performed in ANSYS Workbench. The simulation of the investigated bearing was solved as a linear isotropic material model with given material properties of linear structural steel E = 210,000 MPa, μ = 0.29.

The contact pairs have been customized between the individual roller elements and rings as well as the cage through the contact region function. The contact between the elements was given as friction contact f = 0.2, with a normal stiffness factor of 0.1 and was defined by the Lagrange formula.

The boundary conditions of the bearing have been specified for each part as follows: The outer ring and also inner ring displacement was removed in the z-axis direction and allowed in the direction of the x and y axes in the global Cartesian coordinate system. In the cylindrical global coordinate system, the displacement of the outer ring was taken in the y-direction and allowed in the x-axis and z-axis directions. In the cylindrical global coordinate system, the bead and cage displacement was taken in the x direction and allowed in the y and z direction. The coordinate systems are marked in previous figure (see Fig. 3).

External load was set with value 10,000 N as Bearing Load in the negative y-axis direction with a bearing time of one second for simulation of impact load (see Fig. 4).

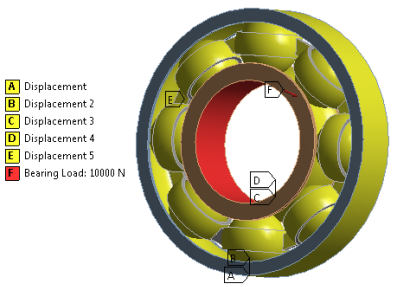

Fig. 4. The boundary conditions of investigated ball bearing

The results of performed FEM analysis with purpose to right investigate and compare analytical and numerical solution of contact characteristics display following Figures. The generated mesh is illustrated in the Fig. 5.

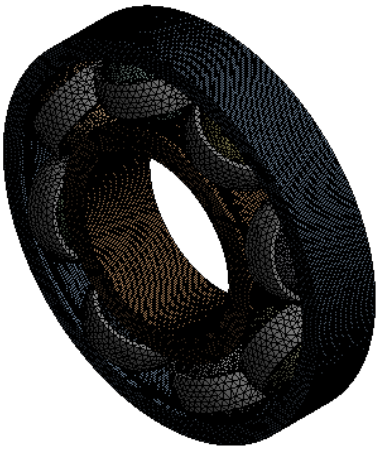

Fig. 5. View of ball bearing generated mesh

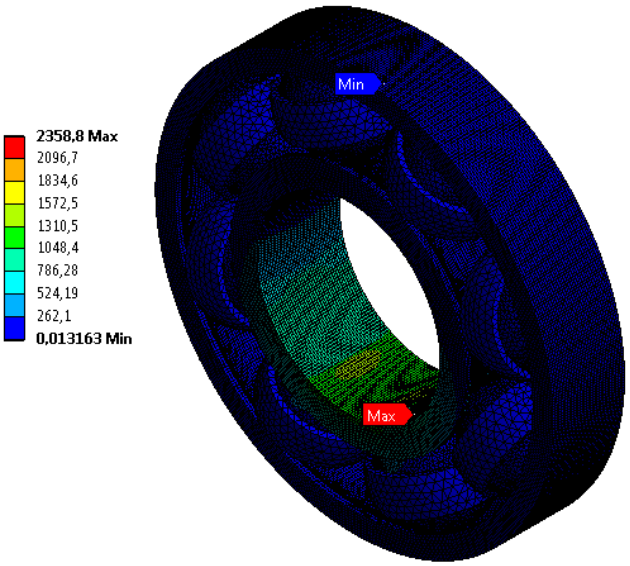

Fig. 6. Equivalent von Mises Stress

From the previous Figures (see Fig. 6-8) is clearly possible to determine value of Equivalent von Mises stress on different parts of investigated rolling bearings. Accordingly is permitted to see the elliptical shape of contact areas and also under surface stresses. Equivalent von-Mises Stress is often used in design work because it allows any arbitrary three-dimensional stress state to be represented as a single positive stress value. Equivalent stress is part of the maximum equivalent stress failure theory used to predict yielding in a ductile material. Equivalent stress is related to the principal stresses by the following equation [11-14].

$$\sigma_e = \left[\frac{(\sigma_1-\sigma_2)^2+(\sigma_2-\sigma_3)^2+(\sigma_3-\sigma_1)^2}{2}\right]^{1/2} \quad (12)$$

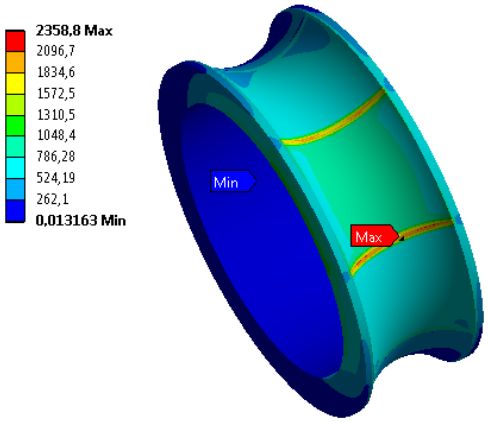

Fig. 7. Equivalent von Mises Stress in detail of inner ring

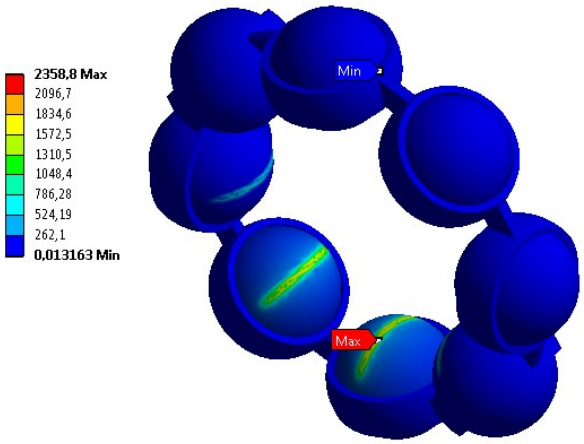

Fig. 8. Equivalent von Mises Stress in detail of rolling elements

From the following Figures (see Fig. 9-11), it is possible to detect the value of contact pressure, contact area and it´s elliptical shape with appropriate parameters *a, b* with corresponding values (a = 5.155, b = 0.361) of rolling elements into orbital paths of bearing rings by the Contact Probe function of Post-processing function.

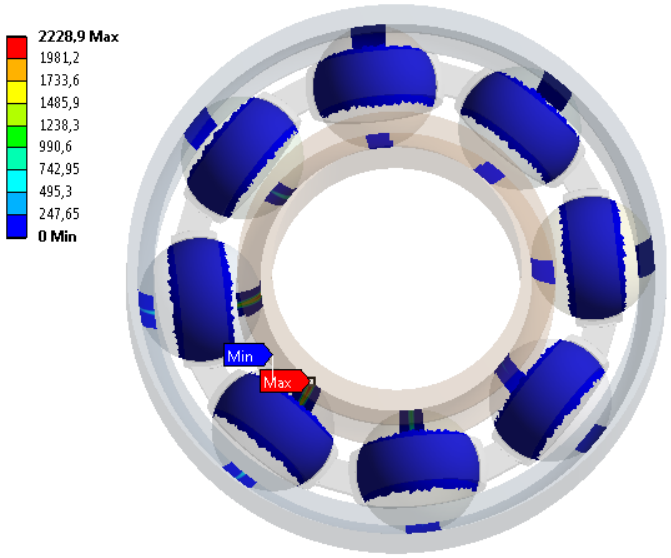

Fig. 9. Maximum contact pressure between rolling element and raceways

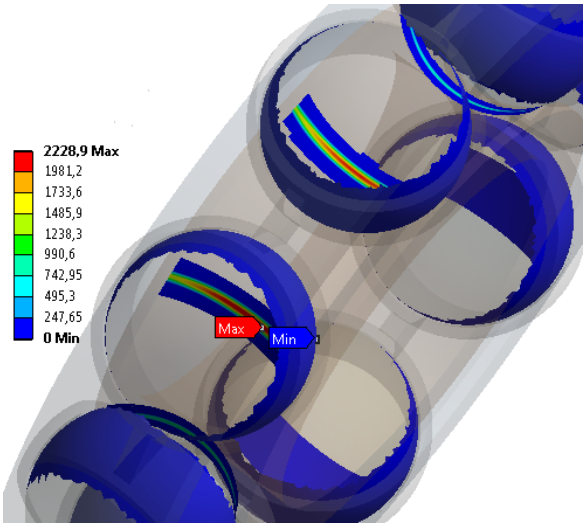

Fig. 10. The detail of contact pressure in contact areas

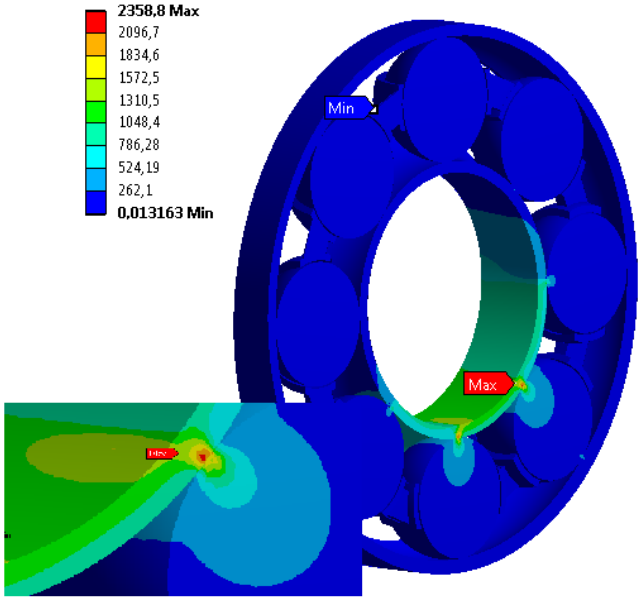

Fig. 11. Maximum contact pressure/Equivalent von Mises Stress between rolling element and raceways in detail of the cut

5 Conclusion

From the simulation and graphical outputs (see Fig. 6-10), the results of the stress-strain analysis using the FEM software can be clearly seen. Through the analysis it was found that the value of the maximum contact pressure gets the size P_{FEM} = 2289.9 MPa (see Fig. 9).

By comparing the results of the analytical and Finite element method (numerical) solutions P_{Hertz} = 2569 MPa = P_{FEM} = 2289.9 MPa**,** it can be detected that the results are almost identical. From the results it is clear that the variation of ANSYS results to that formulated results is very less, that is, less than 11% as percentage deviation.
The results of the MKP analysis are correct, what is proved by comparison of the analytical and numerical solution.

The part of the results of this work has been supported by VEGA grant No. 1/0795/16 and KEGA 017ŽU-4/2017.

References

1. P.K. Gupta, *Computer graphics modeling of rolling bearing dynamics*. Presented at the STLE Annual Meeting, Pittsburg, Pennsylvania (1994)
2. P.R. Anoopath, A.K. Vishwanath, *Hertz contact stress of deep groove ball bearing*. 7th Conference of materials processing and characterization, Published by Elsevier ltd. **5**(1) 3283-3288 (2017)
3. T. Harris, *Rolling Bearings Analysis*. 4th Edition, John-Wiley & Sons Inc., New York (2001)
4. P.M. Johns, R. Gohar, *Roller bearings under radial and eccentric loads*. Tribology International **14**(3) 131-136 (1981)

5. A. B. Jones, *A general theory for elastically constrained ball and radial bearings under arbitrary load and speed conditions*. ASME Journal of Basic Engineering, 309-320 (1960)
6. H. Hertz, *About the contact of elastic bodies*. Collected Works, **1**, Leipzig, Germany (1960)
7. K.L. Johnson, *Contact Mechanics*, Cambridge University Press, Cambridge (1985)
8. M. Dudziak, D. Grzegorz, A. Kolodziej, K. Talaśka, *Contact problems between the hub and the shaft with a four-angular shape of cross-section for different angular positions*. Applied Mechanics and Materials **816**, 54-62 (2015) ISSN 1662-7482
9. V.P. Mateichyk, V.P. Volkov, P.B. Komov, I.V. Gritsuk, *Special features of vehicle condition monitoring using on board diagnostics systems*. Project management, systems analysis and logistics: Scientific journal, K:NTU, **13**, 123-138 (2014)
10. J. Podešva, *The domain of decomposition with the contact problem*. FUIS, V., ed. Engineering Mechanics 2011, 467-470 (2011) ISBN 978-80-87012-33-8
11. L. Jakubovičová, M. Sága, M. Vaško, *Numerical study of influence of mutual slewing of roller bearing rings of the principal stresses at contact area*. Scientific journal of Silesian University of Technology – Series Transport **84**, 83-91 (2014)
12. P. Kopas, M. Sága, V. Baniari, M. Vaško, M. Handrík, *A plastic strain and stress analysis of bending and torsion fatigue specimens in the low-cycle fatigue region using the finite element methods*. Procedia Engineering **177**, 526-531 (2017)
13. T.Y. Božek, Y. Abramov, I.V. Nikitin, R. Yuri, *Reliability determination and diagnostics of a mechatronic system*. Advances in Science and Technology Research Journal **12**, 2, 274-290 (2018)
14. K.E. Václav, Š. Božek, P. Korshunov, A.I. Tarasov, *Numerical analysis of the stress-strain state of a rope strand with linear contact under tension and torsion loading conditions*. Advances in Science and Technology Research Journal **11**, 2, 231-239 (2017) ISSN 2299-8624